Formulation in terms of normalized propagators of a charge-dipole model enabling the calculation of the polarization properties of fullerenes and carbon nanotubes

A. Mayer*
Laboratoire de Physique du Solide, Facultés Universitaires Notre-Dame de la Paix, Rue de Bruxelles 61, B-5000 Namur, Belgium
(Received 5 August 2006; revised manuscript received 5 October 2006; published 8 January 2007)

We present a model for the calculation of the polarization properties of fullerenes and carbon nanotubes. This model describes each atom by both a net electric charge and a dipole. Compared to dipole-only models, the consideration of electric charges enables one to account for the displacement of free electrons in structures subject to an external field. It also enables one to account for the accumulation of additional charges. By expressing the electrostatic interactions in terms of normalized propagators, the model achieves a better consistency as well as an improved stability. In its most elementary form, the model depends on a single adjustable parameter and provides an excellent agreement with other experimental and theoretical data. The technique is applied to a C_{720} fullerene and to open and closed (5,5) nanotubes. The simulations demonstrate the improved stability of our algorithm. In addition, they quantify the role of free charges in the polarization of these structures. The paper finally investigates the field-enhancement properties of open and closed (5,5) nanotubes.

DOI: 10.1103/PhysRevB.75.045407 PACS number(s): 73.63.Fg, 71.20.Tx, 77.22.Ej, 31.15.−p

I. INTRODUCTION

Carbon nanotubes are characterized by exceptional mechanical,[1,2] thermal,[3,4] and electronic[5–7] properties, which make them promising candidates for applications in nanoelectronics.[8,9] Because of their high aspect ratio, these structures turn out to be excellent field emitters as they provide high current densities for macroscopic fields of a few volts per micrometer.[10,11] Carbon nanotubes are also likely to find applications as molecular sensors.[12–14] For the development of these applications, modeling the response of the nanotubes to a macroscopic electric field or to the field due to nearby molecules is therefore an important issue.

First-principles techniques are very useful in this context as they provide accurate atomic and molecular polarizabilities.[15–20] Semiempirical models rely on the data computed by these techniques and enable one to consider larger systems, while reducing the time and computational resources required to address those systems. Because of these reduced computational requirements, semiempirical models are widely used in molecular dynamic simulations, where electrostatic forces have to be computed for every time step, or in problems where many configurations have to be considered.[13] Finally, these models address directly quantities that are of interest for experimentalists: charges and polarization.

A technique traditionally used to describe the polarization of isolated molecules is to associate with each atom a dipole, whose value is computed self-consistently considering the external field and the interactions with the other dipoles.[21–26] In recent publications,[27–29] we extended this description by associating also an electric charge to each atom. This monopole-dipole representation of the electronic densities comes naturally as the Taylor expansion of the charge distribution associated with each atom. The consideration of net charges in sp^2 carbon materials enables one to address the fact that the π electrons of these systems move from one atomic site to the other in response to an external field. It also enables one to account for the accumulation of additional charges, which is essential for the modelization of field emission.[28]

Expanding a recent publication,[30] we present in this paper a formulation in terms of normalized propagators of this charge-dipole representation of nanostructures. This formulation has the advantage of making the model more consistent and of describing more accurately the charge-dipole and the dipole-dipole interactions. It also provides a relation between the extension of the electric charges and the atomic polarizabilities, which reduces the number of adjustable parameters. Compared to our previous formulation,[28] this model is numerically more stable and provides an excellent agreement with other experimental and theoretical data. The details of this technique are presented in Sec. II. The parametrization of the model is given in Sec. III. In Sec. IV, we compare results obtained with a C_{720} fullerene using either our previous model[28] or the current technique. In Sec. V, we then apply the model to open and closed (5,5) nanotubes. The technique provides a consistent definition of the local fields, which enables one to compute the field-enhancement properties of these structures.

II. THEORY: FORMULATION IN TERMS OF NORMALIZED PROPAGATORS OF THE CHARGE-DIPOLE MODEL

We focuss in this paper on sp^2 carbon materials and in particular on fullerenes and carbon nanotubes. Considering the availability of electronic states in the vicinity of the Fermi level (for the structures considered[31–33]) and neglecting quantum-mechanical effects[34] that may prevent electronic charges from moving from one atomic site to the other, we describe each atom by a net charge q_i and a dipole $\mathbf{p}_i$. As explained later, the actual values of the q_i and $\mathbf{p}_i$ will be those that minimize the total electrochemical energy of the system.

A. Total electrochemical energy of a system of charges and dipoles

Let N be the number of atoms in the structure considered. In a reformulation of our previous work,[27–29] the total elec-

trochemical energy E_{tot} associated with a given distribution $\{q_i, \mathbf{p}_i\}$ of charges and dipoles placed at the atomic positions $\mathbf{r}_i$ can be written as

$$E_{\text{tot}} = \frac{1}{2}\sum_{i=1}^{N}\sum_{j=1}^{N} q_i T^{i,j}_{\text{q-q}} q_j - \frac{1}{2}\sum_{i=1}^{N}\sum_{j=1}^{N} \mathbf{p}_i \cdot \mathbf{T}^{i,j}_{\text{p-p}} \mathbf{p}_j - \sum_{i=1}^{N}\sum_{j=1}^{N} \mathbf{p}_i \cdot \mathbf{T}^{i,j}_{\text{p-q}} q_j + \sum_{i=1}^{N} q_i(\chi_i + V_i) - \sum_{i=1}^{N} \mathbf{p}_i \cdot \mathbf{E}, \quad (1)$$

where χ_i stands for the electron affinity of the atom i, V_i refers to the values of the external potential, and $\mathbf{E}$ is the external field.

The physical grounds of Eq. (1) are explained with details in Ref. 28. The first term of this equation accounts for the electrostatic interactions between the charges q_i, the second for the interactions between the dipoles $\mathbf{p}_i$, and the third one for the interactions between the charges and the dipoles (the factor 1/2 prevents the double counting of some of these interactions). The fourth term accounts for the energy required in order to bring a charge q_i to a position characterized by an external potential V_i. It also accounts, through the electron affinity χ_i, for the interactions between the additional charge q_i and the electrons of the atom that stands at the position $\mathbf{r}_i$. The last term finally accounts for the electrostatic interactions between the dipoles $\mathbf{p}_i$ and the external field $\mathbf{E}$.

For a system of point charges, we have $T^{i,j}_{\text{q-q}} = (1/4\pi\epsilon_0) \times (1/r_{i,j})$, with $r_{i,j}$ the distance between the atom i and the atom j. From the elementary definition of a dipole, one can derive the two other tensors using $T^{i,j}_{\text{p-q}} = -\nabla_{\mathbf{r}_i} T^{i,j}_{\text{q-q}} = (1/4\pi\epsilon_0)(\mathbf{r}_{i,j}/r^3_{i,j})$ (with $\mathbf{r}_{i,j} = \mathbf{r}_i - \mathbf{r}_j$) and $T^{i,j}_{\text{p-p}} = -\nabla_{\mathbf{r}_j} \otimes \nabla_{\mathbf{r}_i} T^{i,j}_{\text{q-q}} = (1/4\pi\epsilon_0)(3\mathbf{r}_{i,j} \otimes \mathbf{r}_{i,j} - r^2_{i,j}\mathbf{I})/r^5_{i,j}$ (with $\mathbf{I}$ the 3×3 identity matrix). Consistency with basic electrostatics is verified by the fact that $\mathbf{E}_{q_j} = T^{i,j}_{\text{p-q}} q_j$ provides the electric field due to the charge q_j, while $\mathbf{E}_{\mathbf{p}_j} = T^{i,j}_{\text{p-p}} \mathbf{p}_j$ provides the electric field due to the dipole $\mathbf{p}_j$ (both of them acting on the dipole $\mathbf{p}_i$). The problem when considering point charges is that the tensors $T^{i,j}_{\text{q-q}}$, $\mathbf{T}^{i,j}_{\text{p-q}}$, and $\mathbf{T}^{i,j}_{\text{p-p}}$ diverge as $r_{i,j} \to 0$, so that the term $\mathbf{T}^{i,i}_{\text{p-q}}$ must be removed explicitly while the terms $T^{i,i}_{\text{q-q}}$ and $\mathbf{T}^{i,i}_{\text{p-p}}$ are replaced by finite expressions associated with the self-energy of the charges q_i and of the dipoles $\mathbf{p}_i$, respectively.

B. Description of the charges q_i and of the dipoles $\mathbf{p}_i$ by Gaussian distributions (the Q+P iso [R] model)

In order to solve the difficulties involved with point charges, we assume that the excess charges q_i are described by Gaussian distributions of the form $\rho_i(\mathbf{r}) = (q_i/\pi^{3/2}R^3)\exp(-|\mathbf{r}-\mathbf{r}_i|^2/R^2)$ (with $\mathbf{r}_i$ the position of the atom i and R the width of the distributions). In our previous work,[28] the atomic distances $r_{i,j}$ were replaced by $r_{i,j}/\text{erf}[r_{i,j}/(\sqrt{2}R)]$ in order to make $T^{i,j}_{\text{q-q}}$ exact within that assumption of Gaussian distributions.[35] This renormalization of the distances, however, did not turn $\mathbf{T}^{i,j}_{\text{p-q}}$ and $\mathbf{T}^{i,j}_{\text{p-p}}$ into expressions rigorously correct in that context. The approach developed in this paper consists in considering $T^{i,j}_{\text{q-q}} = (1/4\pi\epsilon_0)\text{erf}[r_{i,j}/(\sqrt{2}R)]/r_{i,j}$ as starting quantity, the components $\mathbf{T}^{i,j}_{\text{p-q}}$ and $\mathbf{T}^{i,j}_{\text{p-p}}$ of the other tensors being determined from the derivation of that expression. It is therefore the tensors $T_{\text{q-q}}$, $\mathbf{T}_{\text{p-q}}$, and $\mathbf{T}_{\text{p-p}}$ themselves that are renormalized, instead of the interatomic distances. Tensors obtained within that renormalization scheme are also referred to as "renormalized propagators" in the literature.[12]

This idea to introduce a factor erf $[r_{i,j}/(\sqrt{2}R)]$ in $T^{i,j}_{\text{q-q}}$ is justified by the fact that $T^{i,j}_{\text{q-q}}$ provides the electrostatic energy of two *Gaussian distributions* of charges, in contrast with that of two *point* charges for which the expressions of the previous section are relevant. These distributions of charges are comparable with the electronic clouds of the carbon atoms and the erf function accounts for the reduction of the electrostatic energy when these clouds interpenetrate. Provided these charge distributions have the form $\rho_i(\mathbf{r}) = (q_i/\pi^{3/2}R^3)\exp(-|\mathbf{r}-\mathbf{r}_i|^2/R^2)$, with $\mathbf{r}_i$ standing for the atomic positions, this treatment is actually exact. The fact that our model relies on an approximation that is physically reasonable (the description of the excess atomic charges by Gaussian distributions) explains why it provides results in good agreement with other theoretical and experimental data (provided the parameters of the model are properly adjusted). Quantum-mechanical effects are expected to become significant in situations where electronic charges are prevented from moving from one atomic site to the other and when considering smaller structures (the quantization of the energy levels is indeed likely to prevent the use of simple classical concepts). For the structures considered in this paper, the energy levels are, however, so close around the Fermi level that classical concepts provide a reasonable approximation.

Developing the idea presented at the beginning this section, we therefore determine

$$\mathbf{T}^{i,j}_{\text{p-q}} = -\nabla_{\mathbf{r}_i} T^{i,j}_{\text{q-q}} = \frac{1}{4\pi\epsilon_0}\frac{\mathbf{r}_{i,j}}{r^3_{i,j}}\left[\text{erf}\left(\frac{r_{i,j}}{\sqrt{2}R}\right) - \sqrt{\frac{2}{\pi}}\frac{r_{i,j}}{R}e^{-r^2_{i,j}/2R^2}\right] \quad (2)$$

and

$$\mathbf{T}^{i,j}_{\text{p-p}} = -\nabla_{\mathbf{r}_j} \otimes \nabla_{\mathbf{r}_i} T^{i,j}_{\text{q-q}} = \frac{1}{4\pi\epsilon_0}\left\{\frac{3\mathbf{r}_{i,j}\otimes\mathbf{r}_{i,j} - r^2_{i,j}\mathbf{I}}{r^5_{i,j}}\left[\text{erf}\left(\frac{r_{i,j}}{\sqrt{2}R}\right) - \sqrt{\frac{2}{\pi}}\frac{r_{i,j}}{R}e^{-r^2_{i,j}/2R^2}\right] - \sqrt{\frac{2}{\pi}}\frac{1}{R^3}\frac{\mathbf{r}_{i,j}\otimes\mathbf{r}_{i,j}}{r^2_{i,j}}e^{-r^2_{i,j}/2R^2}\right\}. \quad (3)$$

In contrast with results obtained by scaling the distances $r_{i,j}$, these two expressions are rigorously correct. $\mathbf{T}^{i,j}_{\text{p-q}}$ describes the electrostatic interactions between a Gaussian distribution of charges q_i and the dipolar moment $\mathbf{p}_j$ associated with Gaussian distributions of charges, while $\mathbf{T}^{i,j}_{\text{p-p}}$ describes the electrostatic interactions between two dipolar moments $\mathbf{p}_i$ and $\mathbf{p}_j$.

The dipolar moments $\mathbf{p}_i$ discussed from this point of the paper can be conceived as two Gaussian distributions of charges, of absolute value $|\mathbf{p}_i|/\Delta x$ and of opposite sign, separated by a distance Δx. In order to reach an infinitesimal

definition of the dipolar moments, one can let Δx tend to zero. The charge density $\rho(\mathbf{r})[\mathbf{p}_i]$ associated with a dipole $\mathbf{p}_i$ is then given by

$$\rho(\mathbf{r})[\mathbf{p}_i] = \lim_{\Delta x \to 0} \frac{|\mathbf{p}_i|/\Delta x}{\pi^{3/2}R^3}\left\{\exp\left[-\left|\mathbf{r}-\left(\mathbf{r}_i+\mathbf{u}\frac{\Delta x}{2}\right)\right|^2/R^2\right] - \exp\left[-\left|\mathbf{r}-\left(\mathbf{r}_i-\mathbf{u}\frac{\Delta x}{2}\right)\right|^2/R^2\right]\right\} = \frac{|\mathbf{p}_i|}{\pi^{3/2}R^3}\mathbf{u}\cdot\nabla\exp(-|\mathbf{r}-\mathbf{r}_i|^2/R^2) = \mathbf{p}_i\cdot\nabla\rho(\mathbf{r})[1], \tag{4}$$

where $\mathbf{u}$ is a unit vector pointing in the direction of the dipole $\mathbf{p}_i$ (from the negative to the positive elementary charge this dipole is made of) and $\rho(\mathbf{r})[1]=(1/\pi^{3/2}R^3)\times\exp(-|\mathbf{r}-\mathbf{r}_i|^2/R^2)$ is the charge density associated with a unit charge on the atom i. From a mathematical point of view, the dipoles $\mathbf{p}_i$ appear naturally associated with the differential operator ∇. From a practical point of view, these dipolar moments $\mathbf{p}_i$ are in essence identical with those encountered in elementary electrostatics, except that the elementary charges $\mathbf{p}_i$ is made of are distributed according to a Gaussian function rather than being point particles.

It can be checked that $\lim_{r_{i,j}\to 0}\mathbf{T}^{i,j}_{\text{p-q}}=0$, which is the result expected by symmetry. The second result is that $\lim_{r_{i,j}\to 0}T^{i,j}_{\text{q-q}}q_i^2/2=\frac{1}{4\pi\epsilon_0}(\sqrt{2/\pi}/R)q_i^2/2$, which is the self-energy of the excess charge q_i already used in our previous work.[27–29] A final noticeable result is that $-\frac{1}{2}\lim_{r_{i,j}\to 0}\mathbf{p}_i\cdot\mathbf{T}^{i,j}_{\text{p-p}}\mathbf{p}_i=\frac{1}{2}\mathbf{p}_i\cdot[(1/4\pi\epsilon_0)(\sqrt{2/\pi}/3R^3)\mathbf{I}]\mathbf{p}_i$, where $\mathbf{I}$ is the 3×3 identity matrix. Since, according to our previous work, this must also be equal to the self-energy $\frac{1}{2}\mathbf{p}_i\cdot\boldsymbol{\alpha}_i^{-1}\mathbf{p}_i$ of the dipole $\mathbf{p}_i$, we find that formulating consistently the interactions within a system of charges and dipoles results in an isotropic atomic polarizability given by

$$\frac{\alpha_{\text{iso}}}{4\pi\epsilon_0} = 3\sqrt{\frac{\pi}{2}}R^3, \tag{5}$$

where R is the width of the charge distributions.

The model is therefore consistent in the sense that the terms $\mathbf{T}^{i,i}_{\text{p-q}}$ cancel naturally while the terms $T^{i,i}_{\text{q-q}}$ and $\mathbf{T}^{i,i}_{\text{p-p}}$ provide the self-energy of the charges and of the dipoles, respectively. The relation (5) constitutes a significant methodological progress. It relates indeed the width of the charge distributions to the atomic polarizabilities, these quantities having been considered as independent in the past. The development also implies that the charges and the dipoles are described by the same extension parameter R, which constitutes the single adjustable parameter of this model (given the positions $\mathbf{r}_i$, the tensors $T_{\text{q-q}}$, $\mathbf{T}_{\text{p-q}}$, and $\mathbf{T}_{\text{p-p}}$ depend on R only). We will refer hereafter to this most elementary form of our model by the notation Q+P iso $[R]$. The Q and P symbols invoke the presence of charges and dipoles in the model. Iso refers to the use of isotropic atomic polarizabilities. The braces contain the adjustable parameters of the model (in this case R, the width of the charge distributions).

C. A first relaxation of the model enabling the charges and the dipoles to be described by different extension parameters (the Q+P iso $[R,\alpha_{\text{iso}}]$ model)

As demonstrated later, the model developed so far provides already an excellent agreement with experimental or other theoretical data. To include, however, additional degrees of freedom in the model, we will relax the Q+P iso $[R]$ model by assuming that the charges q_i and the dipoles $\mathbf{p}_i$ are described by different extension parameters (referred to by R_{q} and R_{p}, respectively). The tensors that determine the total electrochemical energy E_{tot} are then updated according to

$$T^{i,j}_{\text{q-q}}[R_{\text{q-q}}] = \frac{1}{4\pi\epsilon_0}\frac{\text{erf}(r_{i,j}/R_{\text{q-q}})}{r_{i,j}}, \tag{6}$$

$$\mathbf{T}^{i,j}_{\text{p-q}}[R_{\text{p-q}}] = \frac{1}{4\pi\epsilon_0}\frac{\mathbf{r}_{i,j}}{r^3_{i,j}}\left[\text{erf}\left(\frac{r_{i,j}}{R_{\text{p-q}}}\right) - \frac{2}{\sqrt{\pi}}\frac{r_{i,j}}{R_{\text{p-q}}}e^{-(r_{i,j}/R_{\text{p-q}})^2}\right], \tag{7}$$

$$\mathbf{T}^{i,j}_{\text{p-p}}[R_{\text{p-p}}] = \frac{1}{4\pi\epsilon_0}\left\{\frac{3\mathbf{r}_{i,j}\otimes\mathbf{r}_{i,j}-r^2_{i,j}\mathbf{I}}{r^5_{i,j}}\left[\text{erf}\left(\frac{r_{i,j}}{R_{\text{p-p}}}\right) - \frac{2}{\sqrt{\pi}}\frac{r_{i,j}}{R_{\text{p-p}}}e^{-(r_{i,j}/R_{\text{p-p}})^2}\right] - \frac{4}{\sqrt{\pi}}\frac{1}{R^3_{\text{p-p}}}\frac{\mathbf{r}_{i,j}\otimes\mathbf{r}_{i,j}}{r^2_{i,j}}e^{-(r_{i,j}/R_{\text{p-p}})^2}\right\}, \tag{8}$$

where $R_{\text{q-q}}=\sqrt{2}R_{\text{q}}$, $R_{\text{q-p}}=\sqrt{R_{\text{q}}^2+R_{\text{p}}^2}$, and $R_{\text{p-p}}=\sqrt{2}R_{\text{p}}$ are the effective radii relevant to these electrostatic interactions.

In the same way as previously, one can relate the extension R_{p} of the dipoles to an isotropic atomic polarizability given by

$$\frac{\alpha_{\text{iso}}}{4\pi\epsilon_0} = 3\sqrt{\frac{\pi}{2}}R^3_{\text{p}}. \tag{9}$$

Taking this relation into account, this second version of our model depends actually on two parameters: the extension $R=R_{\text{q}}$ of the charge distributions and the isotropic polarizability α_{iso}. We will refer to this model by the notation Q+P iso $[R,\alpha_{\text{iso}}]$. The braces contain the two adjustable parameters of this model. Without the relation (9), α_{iso} and R_{p} would have been considered as two independently adjustable parameters.

D. A second relaxation of the model enabling the consideration of anisotropic polarizabilities (the Q+P aniso $[R,\alpha_{\text{par}},\alpha_{\text{perp}}]$ model)

The model developed so far is intrinsically associated with isotropic atomic polarizabilities. Introducing anisotropic polarizabilities rigorously would require considering from the beginning an anisotropic distribution function for the charges q_i, so that the terms $-\frac{1}{2}\mathbf{p}_i\cdot\mathbf{T}^{i,i}_{\text{p-p}}\mathbf{p}_i$ reduce to $\frac{1}{2}\mathbf{p}_i\cdot\boldsymbol{\alpha}_i^{-1}\mathbf{p}_i$, with $\boldsymbol{\alpha}_i$ anisotropic. We take a simplified approach by just redefining the diagonal elements $\mathbf{T}^{i,i}_{\text{p-p}}$ by $\mathbf{T}^{i,i}_{\text{p-p}}=-\boldsymbol{\alpha}_i^{-1}$, with $\boldsymbol{\alpha}_i$ an anisotropic atomic polarizability tensor arbitrarily associated with the atom i. The tensors $T_{\text{q-q}}$,

$\mathbf{T}_{\text{p-q}}$, and the remaining components of $\mathbf{T}_{\text{p-p}}$ are formally the same as in the previous model.

In order for the relation $-\frac{1}{2}\mathbf{p}_i \cdot \mathbf{T}^{i,i}_{\text{p-p}}\mathbf{p}_i = \frac{1}{2}\mathbf{p}_i \cdot [(1/4\pi\epsilon_0) \times (\sqrt{2/\pi}/3R_{\text{p}}^3)\mathbf{I}]\mathbf{p}_i$ to hold *on average* (for different orientations of the dipole $\mathbf{p}_i$), we enforce that $\alpha_{\text{moy}}/4\pi\epsilon_0 = 3\sqrt{\pi/2}R_{\text{p}}^3$, with the average atomic polarizability α_{moy} related to the main components $(\alpha_{\text{par}}, \alpha_{\text{par}}, \alpha_{\text{perp}})$ of α_i by $\alpha_{\text{moy}} = 3/(2/\alpha_{\text{par}} + 1/\alpha_{\text{perp}})$. These conditions come to enforcing that the trace of $[(1/4\pi\epsilon_0)(\sqrt{2/\pi}/3R_{\text{p}}^3)\mathbf{I}]$ be equal to that of $\boldsymbol{\alpha}_i^{-1}$, so that we achieve the best possible consistency between the intrinsic properties of our model and the atomic polarizability effectively chosen. For the sp^2 carbon materials studied in this paper, α_{par} refers to the components of the atomic polarizability tensor in the plane defined by the three neighbors of a given atom. α_{perp} refers to the component corresponding to the direction perpendicular to that plane. Because of the relation imposed between the extension R_{p} of the dipoles and the components α_{par} and α_{perp} of the polarizability tensor, this last version of our model depends actually on three adjustable parameters: $R = R_{\text{q}}$ (the width of the charge densities), α_{par}, and α_{perp}. This model will be referred to by the notation Q+P aniso $[R, \alpha_{\text{par}}, \alpha_{\text{perp}}]$. Aniso refers to the use of anisotropic atomic polarizabilities. The braces contain the three adjustable parameters of this model.

E. Determination of the actual values of the q_i and $\mathbf{p}_i$ and calculation of the electric potential at an arbitrary position

Given the tensors $T_{\text{q-q}}$, $\mathbf{T}_{\text{p-q}}$, and $\mathbf{T}_{\text{p-p}}$, the total electrochemical energy E_{tot} of the system is entirely determined. The actual values of the charges q_i and of the dipoles $\mathbf{p}_i$ are then obtained by solving the equations $dE_{\text{tot}}/dq_i = 0$, $dE_{\text{tot}}/dp_{x,i} = 0$, $dE_{\text{tot}}/dp_{y,i} = 0$, and $dE_{\text{tot}}/dp_{z,i} = 0$, which minimizes E_{tot}. As explained in Ref. 28, one can enforce that the structure considered carries a net electric charge of Q_{tot} ($Q_{\text{tot}} = 0$ will enforce charge neutrality). The actual values of q_i and $\mathbf{p}_i$ are then obtained by minimizing $f = E_{\text{tot}} + \lambda(\Sigma_{i=1}^{N} q_i - Q_{\text{tot}})$ instead of E_{tot}. One can also account for the presence of a metallic surface, which introduces image interactions within this system of charges and dipoles. The way these interactions must be treated is similar to that presented in Ref. 28.

Finally, once the actual values of the q_i and $\mathbf{p}_i$ are determined, the electric potential $V(\mathbf{r})$ relevant to an electron introduced as test charge at the position $\mathbf{r}$ must be calculated considering the interactions between the gaussian distributions of our model and a point charge. The expression to use for $V(\mathbf{r})$ is then given by

$$V(\mathbf{r}) = V_{\text{ext}}(\mathbf{r}) + \frac{1}{4\pi\epsilon_0}\sum_{i=1}^{N}\left\{\frac{\text{erf}(|\mathbf{r}-\mathbf{r}_i|/R_{\text{q}})}{|\mathbf{r}-\mathbf{r}_i|}q_i + \frac{(\mathbf{r}-\mathbf{r}_i)\cdot\mathbf{p}_i}{|\mathbf{r}-\mathbf{r}_i|^3}\left[\text{erf}\left(\frac{|\mathbf{r}-\mathbf{r}_i|}{R_{\text{p}}}\right) - \frac{2}{\sqrt{\pi}}\frac{|\mathbf{r}-\mathbf{r}_i|}{R_{\text{p}}}e^{-(|\mathbf{r}-\mathbf{r}_i|/R_{\text{p}})^2}\right]\right\}, \tag{10}$$

where the extensions R_{q} and R_{p} of the charge and dipole distributions are used as effective radii for these interactions. $V_{\text{ext}}(\mathbf{r})$ refers to the external potential, which already defined the values V_i at the atomic positions $[V_i = V_{\text{ext}}(\mathbf{r}_i)]$. The electric field $\mathbf{E}(\mathbf{r})$ associated with $V(\mathbf{r})$ is calculated according to the same prescriptions. This expression is more accurate than that proposed in Ref. 28. It is free of divergence. For the modelization of field emission or transport in carbon nanotubes, this expression should be completed by the pseudopotential presented in Ref. 36.

III. PARAMETRIZATION OF THE Q+P ISO [R], OF THE Q+P ISO [R, α_{iso}], AND OF THE Q+P ANISO [$R, \alpha_{\text{par}}, \alpha_{\text{perp}}$] MODELS

From the comparison with other experimental or theoretical data, the parameter R of the Q+P iso [R] model was adjusted to a value of 0.686 203 99 Å, which corresponds to $\alpha_{\text{iso}}/4\pi\epsilon_0 = 1.214\,900\,1$ Å^3. Letting R and α_{iso} be considered as independent parameters, we move to the Q+P iso $[R, \alpha_{\text{iso}}]$ model whose adjusted parameters are $R = 0.672\,001\,49$ Å and $\alpha_{\text{iso}}/4\pi\epsilon_0 = 1.251\,710\,5$ Å^3. It can be noted that, despite the additional degree of freedom introduced in the methodology, the parameters of the Q+P iso $[\text{R}, \alpha_{\text{iso}}]$ model stay close to those of the previous one. Finally, considering anisotropic polarizabilities, we refer to the Q+P aniso $[\text{R}, \alpha_{\text{par}}, \alpha_{\text{perp}}]$ model whose adjusted parameters are $R = 0.663\,294\,37$ Å, $\alpha_{\text{par}}/4\pi\epsilon_0 = 0.544\,966\,47$ Å^3, and $\alpha_{\text{perp}}/4\pi\epsilon_0 = 1.449\,999\,7$ Å^3.

Table I compares the results achieved using these three models with other experimental and theoretical data.[20,22,37–40] The agreement achieved with the Q+P iso [R] model is very satisfactory, considering the fact it depends on a single adjustable parameter. The two other models improve slightly the agreement with the reference data. The improvement achieved by each model (compared to the preceding models) is indicated by an asterisk in Table I. When weighting the absolute deviations between the reference data and the results provided by each model, the Q+P iso [R] model turns out to provide a global error of 5.976, the Q+P iso $[R, \alpha_{\text{iso}}]$ model a global error of 5.305, and the Q+P aniso $[R, \alpha_{\text{par}}, \alpha_{\text{perp}}]$ model a global error of 4.561. For the calculation of these errors, the deviations from the reference data were weighted according to the reliability or the importance we estimated appropriate to associate with each data. The error values presented here were obtained by weighting the deviations from the mean polarizability of C_{60}, C_{70}, and C_{84} by 1/1.5, 1/3, and 1/6, respectively, the deviations from the transverse polarizability of the (5,5), (6,6), and (9,0) nanotubes by 1, and the deviations from the ratio between the internal and external fields in C_{60} and in the (5,5), (6,6), and (9,0) nanotubes by 1/0.025. Deviations related to the (5,5), (6,6), and (9,0) nanotubes were averaged and it is that average that was considered for the calculation of the error function. The values of R, α_{iso}, α_{par}, and α_{perp} provided for each model are those that minimize this error. The fact that the results provided by the three models are only slightly contrasted is due to the domination of the polarization process by the free charges, while the modifications introduced in the

TABLE I. Comparison between experimental and theoretical data and results obtained using the Q+P iso $[R]$, the Q+P iso $[R,\alpha_{iso}]$, and the $Q+P$ aniso $[R,\alpha_{par},\alpha_{perp}]$ models. Data used as target values for the fit are underlined. Improvements provided by each model (compared with the previous models) are indicated with an asterisk. By $\alpha_{\perp}/L$, we mean the lateral polarizability per unit length (infinite nanotubes are considered). By E_{in}/E_{out}, we mean the ratio of internal to external transverse electric fields. The values that serve as reference in these rows were obtained using models where the C_{60} is described by a spherical shell and the nanotubes by cylinders (Ref. 22).

Parameters adjusted for the fit	Q+P iso $[R]$	Q+P iso $[R,\alpha_{iso}]$	Q+P aniso $[R,\alpha_{par},\alpha_{perp}]$	Experimental and theoretical data
Mean polarizability of C_{60} (Å^3)	75.1	75.1	74.5	75.1 (Ref. 20), 76.5±8 (Ref. 37)
Mean polarizability of C_{70} (Å^3)	91.5	91.5	90.9*	89.8 (Ref. 20), 102±14 (Ref. 38), 96.8 (Ref. 39), 107.2 (Ref. 40)
Mean polarizability of C_{84}(Å^3)	116.0	115.9*	115.3*	109.4 (Ref. 20)
$\alpha_{\perp}/L$ of (5,5) nanotubes (Å^2)	8.3	8.3	8.0	8.3 (Ref. 22)
$\alpha_{\perp}/L$ of (6,6) nanotubes (Å^2)	11.3	11.3	11.2*	11.0 (Ref. 22)
$\alpha_{\perp}/L$ of (9,0) nanotubes (Å^2)	8.9	8.9	8.8	8.9 (Ref. 22)
$\alpha_{\perp}/L$ of (12,0) nanotubes (Å^2)	14.5	14.5	14.4*	13.9 (Ref. 22)
$\alpha_{\perp}/L$of (15,0) nanotubes (Å^2)	21.5	21.5	21.4*	20.1 (Ref. 22)
$\alpha_{\perp}/L$ of (18,0) nanotubes (Å^2)	29.9	29.9	29.8*	27.4 (Ref. 22)
E_{in}/E_{out} for C_{60}	0.23	0.25	0.25	0.24 (Ref. 20 and 22)
E_{in}/E_{out} for (5,5) nanotubes	0.14	0.15*	0.22*	0.22 (Ref. 22)
E_{in}/E_{out} for (6,6) nanotubes	0.11	0.11	0.12*	0.22 (Ref. 22)
E_{in}/E_{out} for (9,0) nanotubes	0.13	0.14*	0.14*	0.22 (Ref. 22)

different models deal essentially with the dipoles. The fact that it is the Q+P aniso $[R,\alpha_{par},\alpha_{perp}]$ model that provides the best results confirms the interest of describing the carbon atoms in nanotubes and fullerenes by anisotropic polarizabilities.

In Fig. 1, we represented the axial polarization of a (5,5) nanotube as a function of its length. The results achieved by the three models are perfectly smooth and in excellent agreement with each other. They are also close to the result obtained analytically when representing the nanotube by a metallic cylinder (with a radius 1.2 Å larger than the actual one).[41] This confirms the ability of our model to describe metallic structures (results obtained considering dipoles only are included for comparison). These results also prove the stability of our technique. Compared to our previous work,[28] the current technique is indeed more robust when changing the parameters of the models or the length of the C-C bonds. It has therefore a better ability to deal with structures presenting defects or not built according to purely geometrical considerations. It can thus be applied to the study of large structures, some of them including many defects, in a wide variety of configurations.

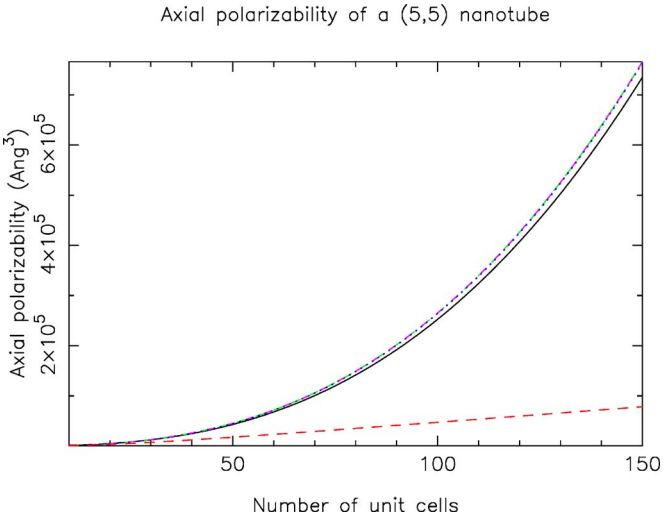

FIG. 1. (Color online) Axial polarizability of a (5,5) nanotube, as obtained analytically with a cylinder (solid) or using the Q+P iso $[R]$ (dashed), the Q+P iso $[R,\alpha_{iso}]$ (dot-dashed), and the Q+P aniso $[R,\alpha_{par},\alpha_{perp}]$ (dotted) models. The lower curve (dashed) stands for results obtained using an anisotropic dipole-only model.

IV. APPLICATION TO THE POLARIZATION OF A C_{720} FULLERENE

In order to demonstrate the improvement achieved in the numerical stability of our technique, we compared in Fig. 2 the results obtained with a C_{720} fullerene using both the previous[28] and the current formulation of our model. The C_{720} fullerene is subject to an external field of 1 V/nm applied horizontally to the left of the figure. The two results are achieved using the Q+P aniso version of each model. The figure actually represents the electric charges as well as the dipoles induced by this external field.

Using the current technique, the molecular polarizability of the C_{720} fullerene is found to be 2135 Å^3. The electric charges contribute to a value of 1999 Å^3 and the dipoles to a value of 136 Å^3. Electric charges provide therefore the main contribution to this polarizability. It can be shown that this contribution grows with the cube of the fullerene radius, while the contribution of dipoles only grows with the square of that radius. The consideration of electric charges is there-

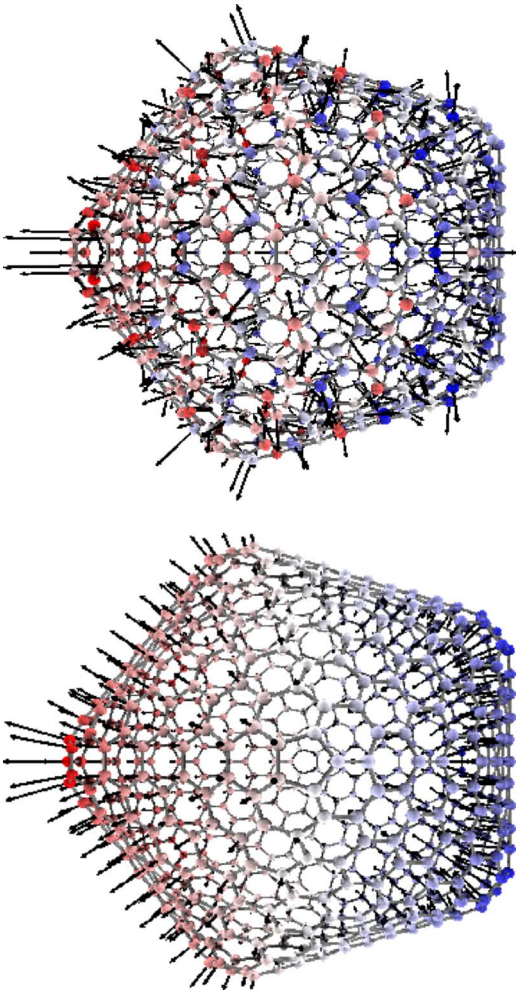

FIG. 2. (Color online) Electric charges and dipoles of a C_{720} fullerene, as induced by a uniform external field of 1 V/nm applied horizontally to the left of the figure. The atoms are represented with a brightness that is proportional to the amplitude of their charge. Positive charges (in red) characterize the left part of the figure, while negative charges (in blue) characterize the right part. Top: the Q+P aniso model of Ref. 28 is used. The minimal and maximal values of the atomic charges are $-9.51\times10^{-3}e$ and $9.50\times10^{-3}e$, respectively (with e the absolute value of the electronic charge). Bottom: the Q+P aniso $[R,\alpha_{\text{par}},\alpha_{\text{perp}}]$ model of this paper is used. The minimal and maximal values of the atomic charges are $-7.75\times10^{-3}e$ and $7.73\times10^{-3}e$, respectively.

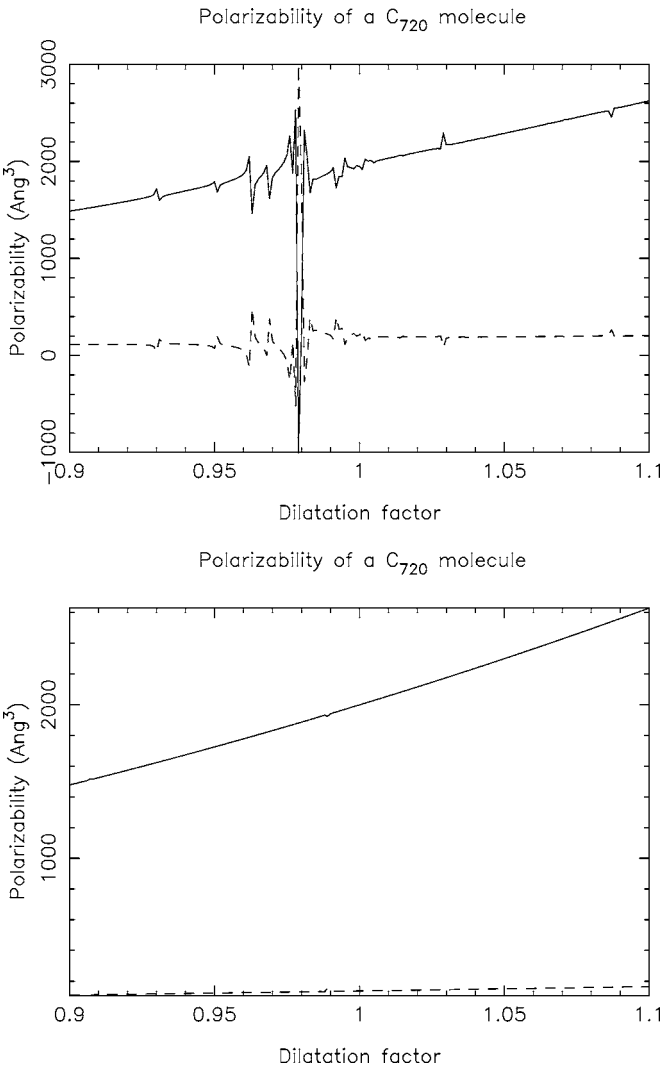

FIG. 3. Polarizability of a C_{720} fullerene, as a function of the dilatation of this molecule (measured by the factor by which the interatomic distances are multiplied). Top: the Q+P aniso model of Ref. 28 is used; Bottom: the Q+P aniso $[R,\alpha_{\text{par}},\alpha_{\text{perp}}]$ model of this paper is used. The solid curve indicates the contribution of charges and the dashed one the contribution of dipoles.

fore essential for the study of these structures. Using our previous formulation of this model,[28] the molecular polarizability is given by 2162 Å^3, the charges and the dipoles contributing 1951 Å^3 and 211 Å^3, respectively.

Although the two formulations provide similar values for the molecular polarizability, the details at the atomic scale are quite different. Figure 2 reveals indeed that the dipoles calculated with the current technique are essentially perpendicular to the surface of the fullerene, with increased values at the corners. This picture is fully consistent with the presence of free electrons, whose equilibrium requires the local fields to be perpendicular to the surface of the fullerene (in this case the dipoles and the local fields point essentially in the same direction). The increased values at the corners of the structure are consistent with the magnification of the local fields at these places. The result also reveals that the distribution of induced charges changes progressively from positive values on the left part of the figure to negative values on the right part. In contrast, the result achieved using the model of Ref. 28 exhibits significant discrepancies with both the charges and the dipoles. These discrepancies are due to the approximations introduced in the charge-dipole and in the dipole-dipole interactions. These interactions are treated more accurately by the current model.

The current model is also less sensitive to the particular geometry of the structure considered. This is illustrated in Fig. 3 where we represented the polarizability of a C_{720} fullerene, whose dimensions are artificially magnified by a factor ranging from 0.9 to 1.1 (compared to the original structure). The result achieved using the model of this paper in perfectly regular, while the result achieved using the pre-

vious version of our model exhibits erratic variations. This proves the better ability of our model, in the form presented in this paper, to deal with a wider variety of structures that are not built according to purely geometrical considerations.

V. APPLICATION TO THE POLARIZATION OF (5,5) CARBON NANOTUBES

The model applies also to carbon nanotubes and gives for these structures the charges and the dipoles that are induced by external fields. It also provides a clear definition of the local fields, which is a useful quantity in field emission. From the polarizability α_i and the dipole $\mathbf{p}_i$ of a given atom, the local fields can indeed be calculated using

$$\mathbf{E}_{\mathrm{loc},i} = \alpha_i^{-1} \cdot \mathbf{p}_i. \tag{11}$$

The effects of the atomic charges are actually contained in the numerical values of the dipoles $\mathbf{p}_i$. To prove the validity of this approach, let us examine the contents of the equation $dE_{\mathrm{tot}}/d\mathbf{p}_i=0$. If we take account of the fact that $\mathbf{T}_{\mathrm{p\text{-}p}}^{i,i}=-\boldsymbol{\alpha}_i^{-1}$ and $\mathbf{T}_{\mathrm{p\text{-}q}}^{i,i}=0$, one can write

$$\frac{dE_{\mathrm{tot}}}{d\mathbf{p}_i} = \boldsymbol{\alpha}_i^{-1}\mathbf{p}_i - \sum_{j\neq i} \mathbf{T}_{\mathrm{p\text{-}p}}^{i,j}\mathbf{p}_j - \sum_{j\neq i} \mathbf{T}_{\mathrm{p\text{-}q}}^{i,j} q_j - \mathbf{E} = 0, \tag{12}$$

which can be put in the form

$$\mathbf{p}_i = \alpha_i \mathbf{E}_{\mathrm{loc},i}, \tag{13}$$

where $\mathbf{E}_{\mathrm{loc},i}=\Sigma_{j\neq i}\mathbf{T}_{\mathrm{p\text{-}p}}^{i,j}\mathbf{p}_j+\Sigma_{j\neq i}\mathbf{T}_{\mathrm{p\text{-}q}}^{i,j}q_j+\mathbf{E}$ is an effective local electric field that accounts for the charges q_j, for the dipoles $\mathbf{p}_j$, and for the external field $\mathbf{E}$. This definition of the local fields has the merit to provide well-defined values. In contrast, the direct calculation of the field due to a collection of point charges or dipoles diverge at the atomic positions. The usual procedure is then to calculate the electric field at a given distance from the emitter. The position at which this field should be calculated is however arbitrary. In our approach, once the charges q_i and the dipoles $\mathbf{p}_i$ have been calculated and independently of the fact charges turn out to dominate the polarization process, the local fields are obtained directly from Eq. (11). It can be noted that the values obtained from the gradient of Eq. (10) are consistent with those provided by Eq. (11). This latter equation is however more concise and easier to implement.

We illustrated this ability of our model to deal with carbon nanotubes by considering a closed (5,5) nanotube standing vertically on a metallic substrate. The cylindrical body of the nanotube consists of 4000 atoms (200 elementary units) and the tube is closed by a half-C_{60} molecule. The tube is subject to a uniform 0.1 V/nm external field applied downwards.

The potential energy, as calculated using Eq. (10), is represented in Fig. 4. For simulations of transport or field emission, this result should be completed by the pseudopotential developed in Ref. 36. The equipotentials represented in Fig. 4 tend to bypass the nanotube, leaving this structure at a nearly constant potential. This is of course the result expected for a metallic structure. The calculation also predicts that the nanotube carries a net electric charge of $-10.8(5)e$,

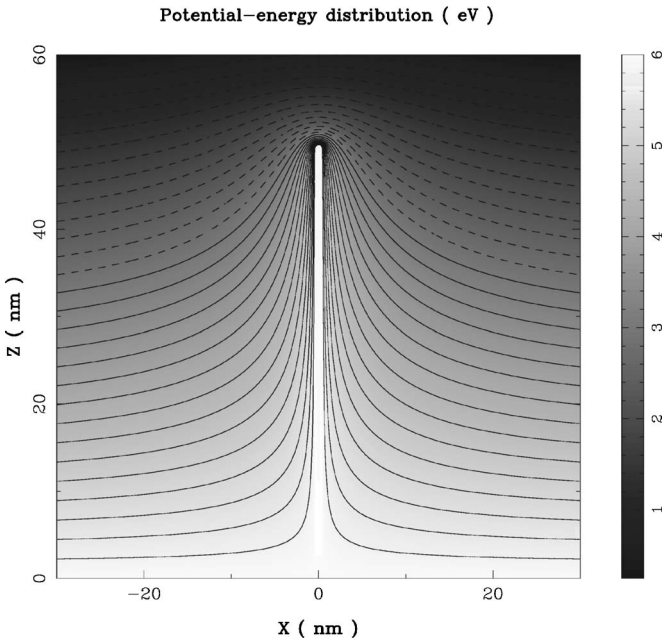

FIG. 4. Potential energy of a closed (5,5) carbon nanotube subject to a uniform 0.1 V/nm external field applied downward. The nanotube consists of 4030 atoms and stands vertically on a metallic substrate. The potential energy is calculated using Eq. (10) in the text.

with e the elementary electric charge. The maximal charge carried by a given atom is as small as $-1.77\times10^{-2}e$. As illustrated in Fig. 5, the maximal values of the atomic charges are achieved at the apex of the nanotube. Net atomic charges are, however, present on the whole body of the nanotube.

Besides the charge q_i and the dipole $\mathbf{p}_i$ of the carbon atoms, another quantity of interest is the local field that acts on these atoms. This quantity is illustrated in Fig. 6, where we represented the local fields at the apex of the closed (5,5) nanotube. The result shows that these local fields keep point-

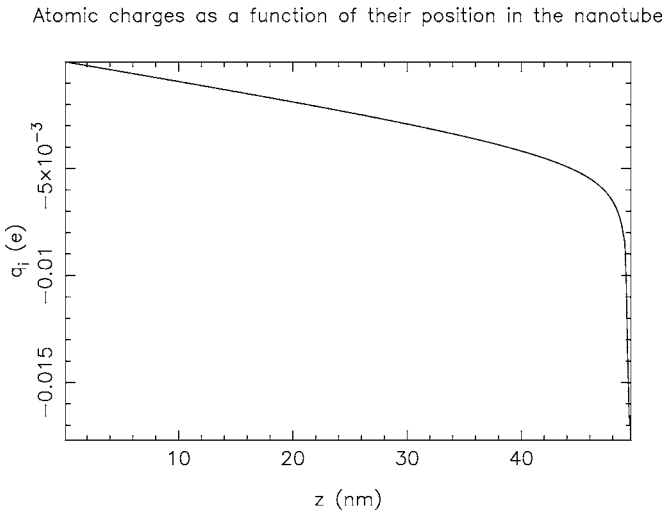

FIG. 5. Net electric charge q_i characterizing the atoms of a closed (5,5) nanotube placed vertically on a metallic substrate and subject to a uniform external field of 0.1 V/nm applied downward.

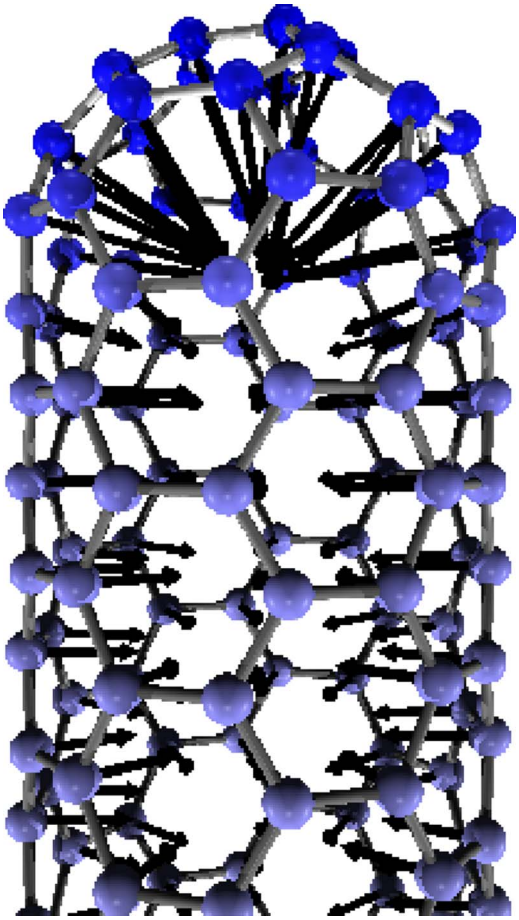

FIG. 6. (Color online) Electric charges and local fields of a closed (5,5) nanotube, as induced by a uniform external field of 0.1 V/nm applied downward. The nanotube stands vertically on a metallic substrate. The atoms are represented with a brightness that is proportional to the amplitude of their charge. The minimal and maximal values of the atomic charges are $-0.177e$ and $-1.25 \times 10^{-4}e$, respectively (with e the absolute value of the electronic charge). This maximal value is not represented on this figure.

ing perpendicularly to the surface of the molecule, both in the body and in the cap of the nanotube. The absolute value of the local fields, for the 4030 atoms of the closed (5,5) nanotube, is represented in Fig. 7. As expected for an elongated structure, the magnitude of the local fields is higher at the apex of the nanotube, where the induced charges were also observed to be higher. Again, the field that acts on the atoms decreases but keeps significant values on the whole body of the nanotube. This is in apparent contradiction with the fact the potential energy in the central axis of the nanotube keeps essentially constant. These local fields are, however, those that act on individual carbon atoms, ensuring that they get polarized in a way that minimizes the total electrostatic energy of the nanotube. These fields are different from those that act on an external electron situated well outside of the atomic charge distributions. This electron is indeed subject to the field exerted by *all* atoms and it was calculated that the field in the center of the nanotube is -1.2×10^{-3} V/nm, which is much smaller than the values represented in Fig. 7 and is consistent with a potential energy

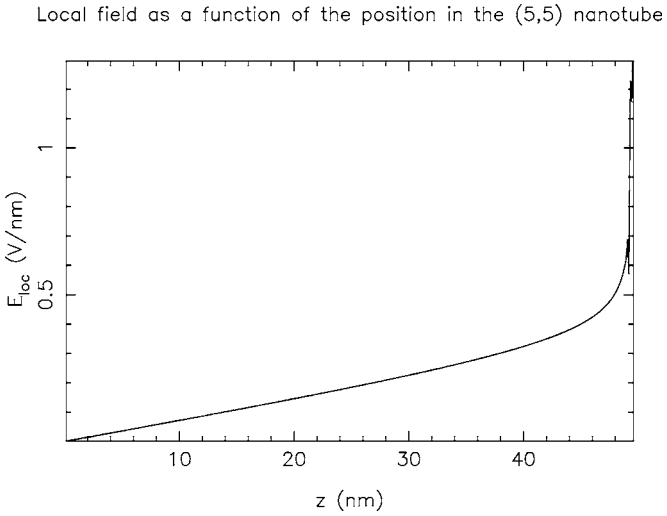

FIG. 7. Local fields characterizing the atoms of a closed (5,5) nanotube placed vertically on a metallic substrate and subject to a uniform external field of 0.1 V/nm applied downward.

keeping essentially constant on the central axis of the nanotube.

The local field at the apex of this closed (5,5) nanotube is 1.30 V/nm, which corresponds to a "field-enhancement factor" $\gamma = E_{\mathrm{loc,max}}/|\mathbf{E}|$ of 13.0 ($E_{\mathrm{loc,max}} = \max_i |\mathbf{E}_{\mathrm{loc},i}|$ and $\mathbf{E}$ is the external macroscopic field). This value is especially important in field-emission theories, because it determines the ability of the structure to emit electrons because of the external field.[42,43] The two other important factors are the emission surface and the work function of the emitter, which can be influenced by adsorbed species thus leading to significant modifications of the emission. The field-enhancement factor is strongly geometry dependent and can thus be controlled by the growing process.

We represented in Fig. 8 the field-enhancement factor γ of open and closed (5,5) nanotubes as a function of their length (expressed by the number of elementary units in the cylindrical body of the nanotube). The results show that the field-enhancement factor of closed (5,5) nanotubes is smaller than that of open ones. Open tubes can therefore be expected to be better field emitters, which agrees with conclusions published previously[44,45] (but not with results published by Bonard *et al.*[46]). The results presented in Fig. 8 can be adjusted by the following two expressions:

$$\gamma_{\mathrm{open}\ (5,5)} = 4.302 + 0.1713\ l/r + \exp\left(-\frac{l/r}{53.30}\right) \times (-3.409 + 7.061 \times 10^{-3}\ l/r), \tag{14}$$

$$\gamma_{\mathrm{closed}\ (5,5)} = 2.004 + 7.596 \times 10^{-2}\ l/r + \exp\left(-\frac{l/r}{53.76}\right) \times (-1.422 + 2.444 \times 10^{-3}\ l/r), \tag{15}$$

where $l = n \times 0.245\ 95$ nm refers to the length of the cylindrical body of the (5,5) nanotube (n is the number of elementary units) and $r = 0.339$ nm to its radius.

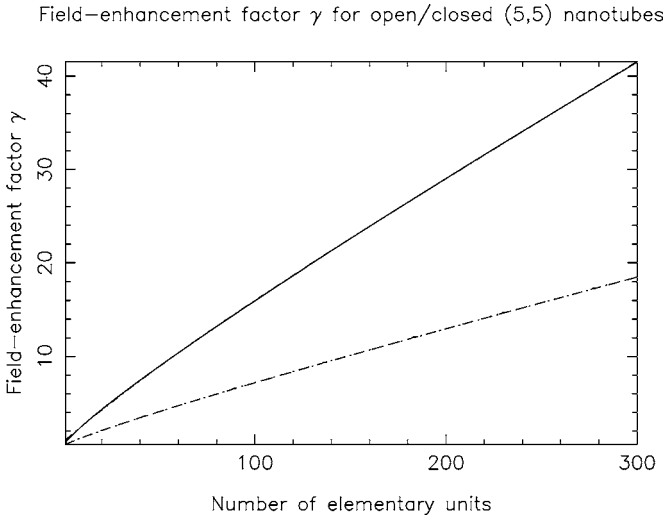

FIG. 8. Field-enhancement factor of open (solid) and closed (dotted) (5,5) carbon nanotubes. These tubes are placed vertically on a metallic substrate. The elementary unit of each nanotube consists of 20 atoms and has a length of 0.245 95 nm. The analytical expressions given by Eqs. (14) and (15) are included as well (they are hardly distinguishable from the numerical results).

These two expressions reproduce the results of Fig. 8 with a mean absolute error of 0.02 (the fits are included in the figure). Furthermore, they agree with long-range expectations (i.e., $\gamma \sim L/r$).[47–50] The proportionality coefficients 0.1713 and 7.596×10^{-2} are, however, smaller than the values of 1,[47] 0.72,[48] or 0.73,[49] found elsewhere. This may come from the small radius of the particular nanotube taken into consideration in this paper ($r=0.339$ nm). Another difference from classical calculations is that the present one is based on an atomistic representation of the nanotube, which does not assume it to be perfectly metallic. The fact that our proportionality coefficient is smaller than values obtained by classical electrostatics is actually in agreement with results published by Peng *et al.*, who performed quantum-mechanical calculations and obtained a proportionality coefficient of 0.2 for closed (5,5) nanotubes.[50] For $l=1$ μm, our formula predicts a field-enhancement factor of 509.6 for open (5,5) nanotubes, which is a realistic value. Finally, compared to previous work, Eqs. (14) and (15) have the advantage of providing also the field-enhancement values corresponding to smaller nanotubes.

VI. CONCLUSION

The applications presented in this paper thus prove the ability of our model to provide results related to the polarization properties of fullerenes and carbon nanotubes with a good accuracy and with reasonable computational resources. Besides improving the calculation of molecular polarization properties (compared to other classical calculations), the technique also gives access to the atomic charges, the atomic dipoles, and the local fields. These quantities turn out to be enhanced at the defects or asperities of these structures, which is likely to influence the dynamics of nearby molecules. The applications also provided an analytical expression for the field-enhancement properties of open and closed nanotubes, which is an important parameter in field emission. Compared to our previous formulation,[28] the model presented in this paper achieves a better consistency as well as a better numerical stability. It provides an excellent agreement with other experimental and theoretical data. Future developments of this model will address the frequency dependence of the parameters as well as nonlinear polarizabilities. In its current form, it constitutes an efficient tool for the systematic study of polarization properties and should help in developing future technologies.

ACKNOWLEDGMENTS

This work was supported by the National Fund for Scientific Research (FNRS) of Belgium. The author acknowledges the use of the Inter-university Scientific Computing Facility (ISCF) and the Belgian State Interuniversity Research Program on "Quantum Size Effects in Nanostructured Materials" (Project No. PAI/IUP P5/01). The author acknowledges M. Devel, R. Langlet, Ph. Lambin, N. M. Miskovsky, and P. H. Cutler for useful discussions.

*Electronic mail: alexandre.mayer@fundp.ac.be

[1] J. N. Coleman, U. Khan, W. J. Blau, and Y. K. Gun'ko, Carbon **44**, 1624 (2006).
[2] J. P. Salvetat, S. Bhattacharyya, and R. B. Pipes, J. Nanosci. Nanotechnol. **6**, 1857 (2006).
[3] H. Rafii-Tabar, Phys. Rep. **390**, 235 (2004).
[4] K. T. Lau, C. Gu, and D. Hui, Composites, Part B **37**, 425 (2006).
[5] M. P. Anantram and F. Leonard, Rep. Prog. Phys. **69**, 507 (2006).
[6] M. S. Dresselhaus, G. Dresselhaus, J. C. Charlier, and E. Hernandez, Philos. Trans. R. Soc. London, Ser. A **362**, 2065 (2004).
[7] M. S. Dresselhaus, G. Dresselhaus, and A. Jorio, Annu. Rev. Mater. Res. **34**, 247 (2004).
[8] R. H. Baughman, A. A. Zakhidov, and W. A. de Heer, Science **297**, 787 (2002).
[9] M. Zhang, S. L. Fang, A. A. Zakhidov, S. B. Lee, A. E. Aliev, C. D. Williams, K. R. Atkinson, and R. H. Baughman, Science **309**, 1215 (2005).
[10] L. Nilsson, O. Gröning, C. Emmenegger, O. Küttel, E. Schaller, L. Schlapbach, H. Kind, J.-M. Bonard, and K. Kern, Appl. Phys. Lett. **76**, 2071 (2000).
[11] V. Filip, D. Nicolaescu, M. Tanemura, and F. Okuyama, Ultramicroscopy **79**, 39 (2001).
[12] R. Langlet, M. Arab, F. Picaud, M. Devel, and C. Girardet, J. Chem. Phys. **121**, 9655 (2004).
[13] M. Arab, F. H. Picaud, M. J-P. Devel, C. Ramseyer, and C. Girardet, Phys. Rev. B **69**, 165401 (2004).
[14] F. Moulin, M. Devel, and S. Picaud, Phys. Rev. B **71**, 165401 (2005).

[15] S. Han and J. Ihm, Phys. Rev. B **61**, 9986 (2000).
[16] C. Kim, B. Kim, S. M. Lee, C. Jo, and Y. H. Lee, Phys. Rev. B **65**, 165418 (2002).
[17] S. Han and J. Ihm, Phys. Rev. B **66**, 241402(R) (2002).
[18] C. Kim, K. Seo, B. Kim, N. Park, Y. S. Choi, K. A. Park, and Y. H. Lee, Phys. Rev. B **68**, 115403 (2003).
[19] X. Zheng, G. H. Chen, Z. Li, S. Deng, and N. Xu, Phys. Rev. Lett. **92**, 106803 (2004).
[20] D. Jonsson, P. Norman, K. Ruud, H. Ågren, and T. Helgaker, J. Chem. Phys. **109**, 572 (1998).
[21] Ch. Girard, Ph. Lambin, A. Dereux, and A. A. Lucas, Phys. Rev. B **49**, 11425 (1994).
[22] L. X. Benedict, S. G. Louie, and M. L. Cohen, Phys. Rev. B **52**, 8541 (1995).
[23] P. A. Gravil, Ph. Lambin, G. Gensterblum, L. Henrard, P. Senet, and A. A. Lucas, Surf. Sci. **329**, 199 (1995).
[24] P. A. Gravil, M. Devel, Ph. Lambin, X. Bouju, Ch. Girard, and A. A. Lucas, Phys. Rev. B **53**, 1622 (1996).
[25] M. Devel, Ch. Girard, and Ch. Joachim, Phys. Rev. B **53**, 13159 (1996).
[26] A. Mayer and J.-P. Vigneron, Phys. Rev. B **56**, 12599 (1997).
[27] A. Mayer, Appl. Phys. Lett. **86**, 153110 (2005).
[28] A. Mayer, Phys. Rev. B **71**, 235333 (2005).
[29] A. Mayer and Ph. Lambin, Nanotechnology **16**, 2685 (2005).
[30] A. Mayer, Ph. Lambin, and R. Langlet, Appl. Phys. Lett. **89**, 063117 (2006).
[31] R. Saito, M. Fujita, G. Dresselhaus, and M. S. Dresselhaus, Appl. Phys. Lett. **60**, 2204 (1992).
[32] R. Saito, G. Dresselhaus, and M. S. Dresselhaus, J. Appl. Phys. **73**, 494 (1993).
[33] J.-C. Charlier and Ph. Lambin, Phys. Rev. B **57**, R15037 (1998).
[34] X. Zhou, H. Chen, and O.-Y. Zhong-can, J. Phys.: Condens. Matter **13**, L635 (2001).
[35] L. Jensen, P.-O. Åstrand, A. Osted, J. Kongsted, and K. V. Mikkelsen, J. Chem. Phys. **116**, 4001 (2002).
[36] A. Mayer, Carbon **42**, 2057 (2004).
[37] R. Antoine, Ph. Dugourd, D. Rayane, E. Benichou, F. Broyer, M. Chandezon, and C. Guet, J. Phys. Chem. **110**, 9771 (1999).
[38] I. Compagnon, R. Antoine, M. Broyer, P. Dugourd, J. Lermé, and D. Rayane, Phys. Rev. A **64**, 025201 (2001).
[39] S. L. Ren, K. A. Wang, P. Zhou, Y. Wang, A. M. Rao, M. S. Meier, J. P. Selegue, and P. C. Eklund, Appl. Phys. Lett. **61**, 124 (1992).
[40] A. F. Hebard, R. C. Haddon, R. M. Fleming, and A. R. Kortan, Appl. Phys. Lett. **59**, 2109 (1991).
[41] L. D. Landau, E. M. Lifshitz, and L. P. Pitaesvkii, *Electrodynamics of Continuous Media* (Pergamon, Oxford, 1981).
[42] R. H. Fowler and L. Nordheim, Proc. R. Soc. London, Ser. A **119**, 173 (1928).
[43] R. H. Good and E. Müller, *Field Emission* Handbüch der Physik Vol. 21 (Springer-Verlag, Berlin, 1956), pp. 176–231.
[44] A. G. Rinzler, J. H. Hafner, P. Nicolaev, L. Lou, S. G. Kim, D. Tomanek, P. Nordlander, D. T. Colbert, and R. E. Smalley, Science **269**, 1550 (1995).
[45] A. Mayer, N. M. Miskovsky, P. H. Cutler, and Ph. Lambin, Phys. Rev. B **68**, 235401 (2003).
[46] J. M. Bonard, J. P. Salvetat, T. Stockli, L. Forro, and A. Chatelain, Appl. Phys. A: Mater. Sci. Process. **69**, 245 (1999).
[47] R. V. Latham, *High Voltage Vacuum Insulation: The Physical Basis* (Academic, London, 1981).
[48] C. J. Edgcombe and U. Valdre, Solid-State Electron. **45**, 857 (2001).
[49] G. C. Kokkorakis, A. Modinos, and J. P. Xanthakis, J. Appl. Phys. **91**, 4580 (2002).
[50] J. Peng, Z. Li, C. He, S. Deng, N. Xu, X. Zheng, and G. Chen, Phys. Rev. B **72**, 235106 (2005).